Available online at www.sciencedirect.com
ScienceDirect
Journal of Magnetic Resonance 186 (2007) 94–99
JMR Journal of Magnetic Resonance
www.elsevier.com/locate/jmr

Resolution enhancement using a new multiple-pulse decoupling sequence for quadrupolar nuclei

L. Delevoye [a,*], J. Trébosc [a], Z. Gan [b], L. Montagne [a], J-P. Amoureux [a]

[a] UCCS, CNRS-8181, ENSCL-USTL, 59652 Villeneuve d'Ascq, France
[b] NHMFL, 32310 Tallahassee, FL, USA

Received 8 December 2006; revised 25 January 2007
Available online 31 January 2007

Abstract

A new decoupling composite pulse sequence is proposed to remove the broadening on spin $S = 1/2$ magic-angle spinning (MAS) spectra arising from the scalar coupling with a quadrupolar nucleus I. It is illustrated on the ^{31}P spectrum of an aluminophosphate, $AlPO_4$-14, which is broadened by the presence of $^{27}Al/^{31}P$ scalar couplings. The multiple-pulse (MP) sequence has the advantage over the continuous wave (CW) irradiation to efficiently annul the scalar dephasing without reintroducing the dipolar interaction. The MP decoupling sequence is first described in a rotor-synchronised version (RS-MP) where one parameter only needs to be adjusted. It clearly avoids the dipolar recoupling in order to achieve a better resolution than using the CW sequence. In a second improved version, the MP sequence is experimentally studied in the vicinity of the perfect rotor-synchronised conditions. The linewidth at half maximum (FWHM) of 65 Hz using ^{27}Al CW decoupling decreases to 48 Hz with RS-MP decoupling and to 30 Hz with rotor-asynchronised MP (RA-MP) decoupling. The main phenomena are explained using both experimental results and numerical simulations.

Keywords: Solid-state NMR; Quadrupolar nuclei; Decoupling; Scalar coupling

1. Introduction

Spin decoupling is one of the most common procedure that is used in NMR. In liquid-state NMR, the spectral linewidth is often not controlled by the relaxation of the observed nucleus but rather by the *J*-couplings. For organic solutions, one usually decouples the isotropic heteronuclear *J*-coupling by applying either a multiple-pulse sequence (GARP [1] or SEDUCE-3 [2]) or adiabatic pulses (WURST [3]). Broadband heteronuclear decoupling is easy to achieve at relatively low rf-field amplitudes due to the fact that *J*-coupling constants are often quite small. Moreover, the dipolar couplings in solution are naturally removed by a rapid tumbling of the molecules. In inorganic solution, the observed nucleus can be chemically bonded to a quadrupolar nucleus with a spin number $I > 1/2$. If the bonded quadrupolar nucleus is of high natural abundance, the spectrum is then composed of a $2nI + 1$ multiplet, where n is the number of bonded nuclei. ^{51}V and ^{93}Nb ^1J couplings have been reported to affect the ^{17}O spectral resolution [4]. The effects of decoupling schemes have been investigated in the case of ^{13}C [5] and ^1H [6] coupled to ^2H and ^{10}B, respectively.

In solid-state NMR, the spectral linewidth of spin-1/2 nuclei is dominated by the heteronuclear dipolar broadening with a neighbouring nucleus of high natural abundance. Due to strong homonuclear dipolar couplings, heteronuclear decoupling sequences are necessary and thus contribute to increase the resolution of these nuclei. Originally, ^1H continuous wave (CW) decoupling was used during the acquisition of spectra to remove the heteronuclear dipolar coupling with protons. The CW decoupling is now commonly replaced in NMR of rotating solids by efficient broadband decoupling sequences like TPPM [7], XiX [8], SPINAL [9] and others [10–16]. These decoupling

* Corresponding author.
E-mail address: laurent.delevoye@ensc-lille.fr (L. Delevoye).

1090-7807/$ - see front matter © 2007 Elsevier Inc. All rights reserved.
doi:10.1016/j.jmr.2007.01.018

patterns all involve a continuous irradiation of the protons with repeating pulses of equal length but with a complex rf-phase cycle. A new method called PIPS [17], using rotor-synchronised π pulses has also been proposed for spin-1/2. Orr and Duer [18] have also recently used ^{14}N adiabatic pulses to improve the ^{13}C resolution. It is important to note that all these sequences are dedicated to annul the dipolar dephasing. Scalar couplings between spin-1/2 and a quadrupolar nucleus have been observed on solid-state NMR spectra of the spin-1/2 and measurements of ^1J and ^2J couplings have been made on a wide variety of spin pairs [19–24]. Recently, we have demonstrated that a ^2J ^{31}P–^{27}Al bonding could dramatically broaden the ^{31}P spectrum of well-crystallised compounds [25]. The CW decoupling of quadrupolar nuclei connected to the observed spin-1/2 nuclei had been proposed, with soft rf field, due to a strong dipolar recoupling at high rf field. In this article, we propose new improved methods, based on multiple-pulse decoupling, to further improve the resolution of these spin-1/2 nuclei.

2. Experimental

All experiments were performed at a MAS spinning rate of $\nu_R = 10$ kHz, on a 9.4 T spectrometer equipped with a 3.2 mm triple-resonance CPMAS probe, operating at ^1H, ^{27}Al and ^{31}P of 400.13, 104.3 and 161.7 MHz, respectively. The as-synthesized aluminophosphate $AlPO_4$-14, with isopropylamine template, was used as a test compound to demonstrate the efficiency of the different decoupling sequences. It has 4 crystallographic ^{31}P sites, each connected to ^{27}Al sites through four P–O–Al bonds [25,26]. A cross-polarisation (CP) from the protons was used to generate the initial ^{31}P signal, immediately followed by data acquisition under simultaneous ^1H (TPPM) and ^{27}Al (CW, RS-MP or RA-MP) decouplings. Decoupling rf-field amplitudes were set to the arcing limit of the probehead, i.e. 90 and 70 kHz for ^1H and ^{27}Al, respectively, except when it is clearly mentioned. ^{31}P chemical shift is given in ppm with respect to external 85% H_3PO_4.

Simulations were carried out with the SIMPSON program provided by Bak et al. [27]. They were run on a cluster computer of ten 2 GHz AMD CPUs. The considered spin system was composed of one ^{27}Al nucleus with a quadrupolar interaction of $C_Q = 3$ MHz, $\eta_Q = 0$ simulated to the 2nd order on the decoupled channel and one ^{31}P nucleus on the observed channel of a spectrometer whose ^1H Larmor frequency is 400 MHz. The two nuclei were coupled through either a dipolar coupling $D = 500$ Hz or an isotropic coupling $J = 30$ Hz or both interactions together. Quadrupolar and dipolar tensors were aligned. Simulations of systems including two ^{27}Al were too long to perform especially for RA-MP. Spinning rate was 10 kHz; the simulated FIDs were about 40 ms long and spectral width was around 10 kHz. The FIDs were Fourier transformed using 50 Hz apodization and the maxima of the corresponding spectra were used to plot the figures.

3. Results and discussion

In this contribution, we propose a new high-power decoupling sequence of quadrupolar nuclei which leads to a significant improvement in decoupling performance compared to CW decoupling. The new sequence, sketched in Fig. 1b, consists of a series of rf pulses of amplitude ν_1^{Al} and length τ_p separated by a delay τ_d. The decoupling sequence can be used in a rotor-synchronised mode (RS-MP) by choosing $\tau_p + \tau_d = \tau_R$ where τ_R stands for the rotor period. The use of short pulses separated by long delays ($\tau_d = 85$ μs) in the RS-MP decoupling sequence is justified by the difference in magnitude of the $^{27}Al/^{31}P$ dipolar and scalar couplings. Indeed, the scalar dephasing being much slower than the dipolar one, there is no need for a continuous irradiation for an efficient scalar decoupling. We will further consider an asynchronised improved version of the MP decoupling sequence (RA-MP) by letting $\tau_p + \tau_d$ values deviating slightly from the rotor period.

Fig. 2 shows a restricted region (P_1 and P_4) of the ^{31}P spectra of $AlPO_4$-14 obtained under different ^{27}Al decoupling conditions. In Fig. 2a, the resolution comes from the application of a CW decoupling pulse of optimal rf field strength of $\nu_1^{Al} = 15$ kHz. The spectral resolution (FWHM) of ca. 65 Hz is close to the one observed in our previous work [25]. The RS-MP and RA-MP decoupling sequences (Figs. 2b and c) lead to a large improvement of the spectral resolution with linewidths of 48 and 38 Hz, respectively, at the optimal experimental conditions. It is important to note that the ^{27}Al rf field amplitude (70 kHz) was set to the maximum power that the probehead could undergo under the RS-MP experimental conditions (decoupling duty cycle of 15%). The spectrum in Fig. 2d was obtained with an optimized RA-MP decoupling. The decoupling duty cycle is then shorter (4%), which allowed using an increased ^{27}Al rf field of 90 kHz. In this case, the spectral linewidth decreases to reach 30 Hz, only.

3.1. Rotor-synchronised multiple-pulse decoupling

Fig. 3a compares the evolution of the ^{31}P linewidth in the conditions of CW (plain circles) or RS-MP (grey upside-down triangles) ^{27}Al decouplings. The CW decou-

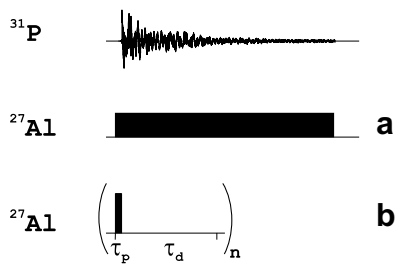

Fig. 1. Sketch of the CW (a) and MP (b) decoupling sequences. Under MP decoupling, the quadrupolar nuclei are irradiated every delay τ_d with pulses of equal width τ_p and following a XY-16 phase cycling scheme [30]. The ^{31}P excitation is preceded by a CP transfer from the ^1H.

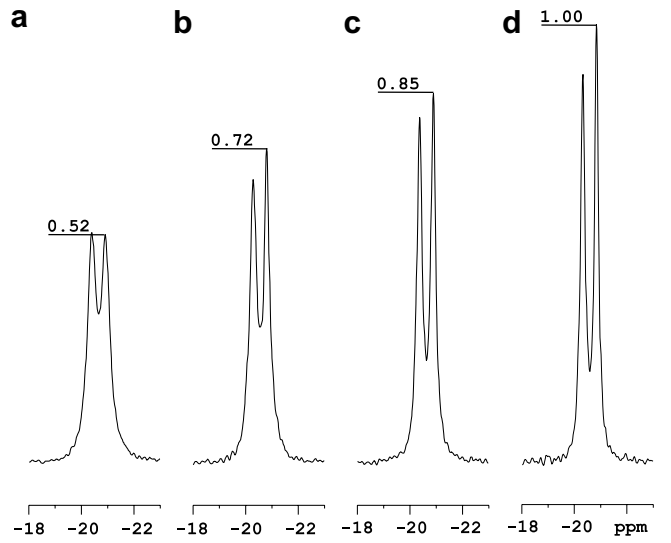

Fig. 2. The P_4 (−20.34 ppm) and P_1 (−20.85 ppm) resonances of $AlPO_4$-14 under different ^{27}Al decoupling conditions and rf field amplitudes, at a spinning speed of 10 kHz. (a) CW decoupling at $\nu_1^{Al} = 15$ kHz, (b) RS-MP decoupling at $\nu_1^{Al} = 70$ kHz ($\tau_p = 15$ μs and $\tau_d = 85$ μs), (c) RA-MP decoupling at $\nu_1^{Al} = 70$ kHz ($\tau_p = 6$ μs and $\tau_d = 100$ μs) and (d) RA-MP at $\nu_1^{Al} = 90$ kHz ($\tau_p = 4$ μs and $\tau_d = 100$ μs).

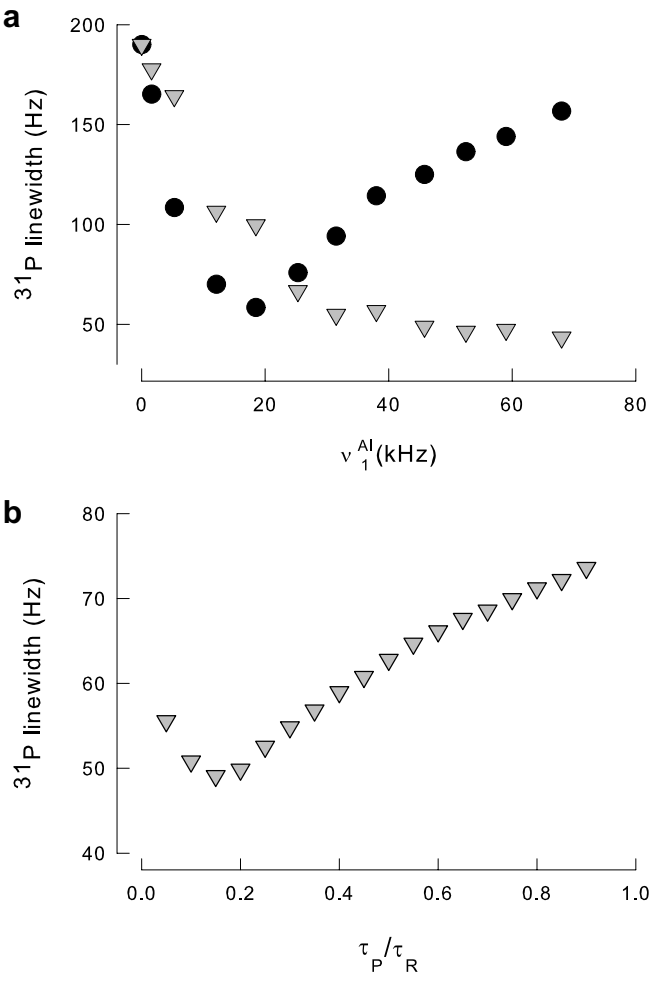

Fig. 3. Variation of the ^{31}P linewidth of site P_4 in $AlPO_4$-14, versus (a) the ^{27}Al rf field strength using different decoupling schemes (CW and RS-MP) and (b) the optimisation of the τ_p/τ_R parameter under RS-MP decoupling. Plain circles correspond to CW decoupling data and grey upside-down triangles stand for RS-MP decoupling data with (a) $\tau_p = 15$ μs and $\tau_d = 85$ μs and (b) $\nu_1^{Al} = 70$ kHz.

pling, as previously published [25], leads to 2 regions where the resolution evolves in different directions. For low ^{27}Al rf field, the ^{31}P linewidth improves due to an efficient decoupling of the ^{27}Al/^{31}P scalar couplings. But, in a second regime ($\nu_1^{Al} > 15$ kHz), the ^{31}P linewidth dramatically increases under the effect of the recoupling of the ^{27}Al/^{31}P dipolar interactions. The dipolar recoupling of a spin pair, which involves a quadrupolar nucleus, has been investigated in the case of the development of the transfer of population double-resonance (TRAPDOR) sequence [28]. In this sequence, the strong irradiation of the quadrupolar nucleus during the spin echo on observe nucleus, prevents the refocusing of the dipolar coupling under MAS conditions. Through a simplistic model [25] which takes into account the dipolar coupling only, we previously demonstrated that a similar situation occurs during the ^{27}Al irradiation decoupling. We further showed that the ^{27}Al strong CW irradiation during ^{31}P acquisition had a negative impact on the spectral resolution.

On the other hand, the evolution of the ^{31}P linewidth in the RS-MP case (grey upside-down triangles) decreases monotonously in function of the rf field increase. In other words, the experimental data reveal no apparent recoupling of the dipolar interaction with the decoupling rf field. In Fig. 3b, the ^{31}P linewidth is recorded in function of the τ_p/τ_R ratio. The choice of synchronising the decoupling pulses on the rotor period is justified by the fact that synchronisation makes it less probable that the pulses annul the decoupling effect of MAS on the dipolar interactions. This procedure is furthermore interesting because the synchronising process renders the decoupling sequence very easy to optimise. Here, only the τ_p/τ_R ratio needs to be experimentally set, the rf amplitude ν_1^{Al} being set at the maximum possible value (see Fig. 3a). In our case, the optimal ^{31}P resolution is obtained for a ratio of 0.15. As it was the case for the REAPDOR experiment [29], even short ^{27}Al pulses induce a certain amount of adiabatic transfers that lead to some dipolar recoupling. Most probably, the optimal ratio of 0.15 is the result of a situation where the dipolar recoupling is in competition with scalar decoupling. It is important to note, that in other Al–O–P experimental cases, on various samples, we have always reached the best resolution for a τ_p/τ_R ratio in a range from 0.1 and 0.2.

3.2. Offset and Bloch–Siegert shift

In Fig. 4, we compare two important experimental parameters for both the CW and the RS-MP decoupling: the influence of the ^{27}Al offset on the ^{31}P resolution (Figs. 4a and b) and the influence of the ^{27}Al rf field amplitude on

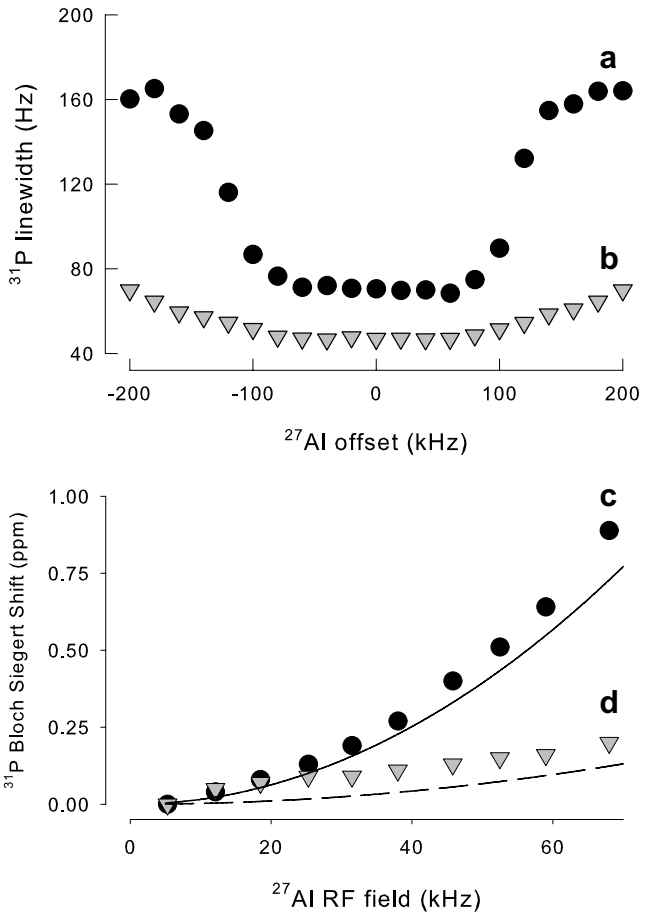

Fig. 4. (a) and (b) Variation of the ^{31}P linewidth versus the ^{27}Al offset and (c) and (d) Bloch–Siegert shift versus the ^{27}Al rf field amplitude. Data were obtained with CW (plain circles) and RS-MP (grey upside-down triangles) decoupling sequences. The full and dashed lines represent the calculated functions as expressed in Eq. (1) and scaled by 0.15, respectively.

the ^{31}P resonance frequency (Figs. 4c and d). In Fig. 4a, the plain circles correspond to the data points obtained with the CW decoupling sequence. This experiment was run with the optimum ^{27}Al rf field amplitude ($\nu_1^{Al} = 15$ kHz) that was presented in Fig. 3a. It is clear that when the ^{27}Al offset is greater than 100 kHz, the resolution is quickly lost. This is directly related to the fact that the optimum decoupling is in the range of small rf fields. Hence, in addition to potentially recoupling the dipolar interaction, the CW decoupling has a strong offset dependence. However, the RS-MP decoupling, which requires high rf fields with short durations, has very little offset dependence. This is clearly observable in Fig. 4b. The RS-MP decoupling sequence has been used with a XY-16 phase cycling [30] that in previous studies, has revealed to decrease the offset dependence. The comparison of the XY-16 phase cycling and simpler ones, has shown a slight difference in offset dependence in favor of the XY-16 one.

Fig. 4c and d shows the relation between ^{31}P resonance frequency and ^{27}Al rf field amplitude. One can observe that for both decoupling schemes, the position of the resonance is shifted as the ^{27}Al rf field increases. This effect, i.e. the Bloch–Siegert shift [31], occurs when an off-resonance oscillating rf irradiation contributes to shift the resonance frequency of an observed nucleus. In the context of decoupling, this off-resonance field is the hetero-nuclear decoupling field ν_1^{Al}. According to reference [32], in case of a CW decoupling, the Bloch–Siegert shift can be expressed (in ppm) as

$$\left(\frac{\gamma_p}{\gamma_{Al}}\right)^2 \frac{(\nu_1^{Al})^2}{(\nu_0^{P})^2 - (\nu_0^{Al})^2} \times 10^6 \quad (1)$$

where γ_p and γ_{Al} are the ^{31}P and ^{27}Al gyromagnetic ratios, ν_1^{Al} is the ^{27}Al rf field strength and ν_0^{P} and ν_0^{Al} are the ^{31}P and ^{27}Al Larmor frequencies.

The data points that were obtained through CW decoupling reveal an important shift in ^{31}P in function of the ^{27}Al rf field. The full line curve calculated with Eq. (1) is a close fit to the data. However, the best rf field for the CW decoupling is smaller than 20 kHz, which limits significantly the Bloch–Siegert effect. In the case of the RS-MP decoupling (grey upside-down triangles), the Bloch–Siegert effect is relatively small across the entire range of rf field. Indeed, the Bloch–Siegert effect only occurs during the decoupling pulse. In our case, this corresponds to only 15% of the ^{31}P acquisition time, and thus to the dashed curve in Fig. 4d. Hence, even if small, the deviations caused by the Bloch–Siegert effect must be considered and corrected.

3.3. Rotor-asynchronised multiple-pulse decoupling

In this last section, we will study the ^{31}P resolution under conditions that are close to the synchronisation optimum. Surprisingly, the condition of perfect synchronisation that we presented in the previous sections and that revealed better results than the classic CW decoupling procedure, corresponds to the minimum intensity in Fig. 5.

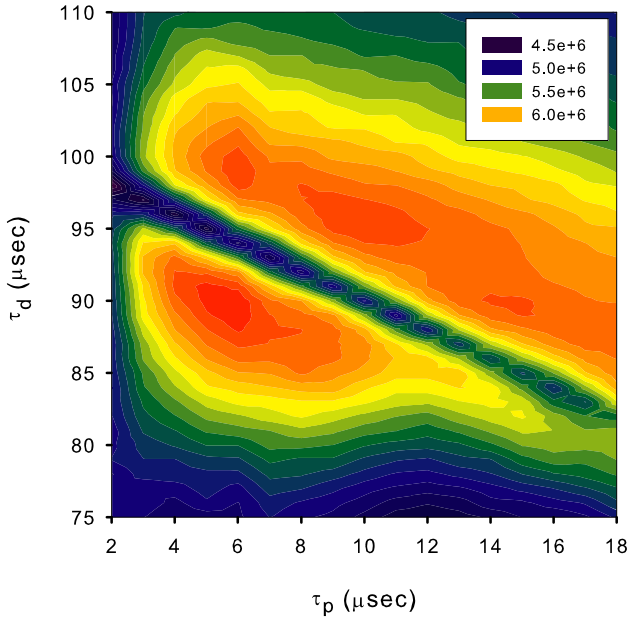

Fig. 5. Experimental intensity of site P_4 versus τ_d and τ_p ($\nu_1^{Al} = 70$ kHz).

This was observed for each value of τ_p. The maximum of amplitude is found at values close to exact synchronisation, but on either side of the dip. For the experimental case of site P_4 in the $AlPO_4$-14, the maximum intensity is obtained for τ_p and τ_d of 6 and 100 μs, respectively. The other sites are characterized by similar curve patterns with a dip at the synchronisation condition. If one were to consider the dipolar interactions only, one would expect the synchronisation condition to lead to a peak in intensity. This is indeed what is observed in Fig. 5, if one puts aside the very narrow but strong dip found at the value of exact synchronisation. Overall, this pattern of results lead us to consider the presence of another phenomenon.

In a second step, a series of simulations were conducted in order to try and reproduce those experimental results of Fig. 5. The first calculation is presented in Fig. 6a. Here, the calculation was run with the ^{31}P–^{27}Al spin system that underwent a dipolar coupling only, of magnitude 500 Hz, which corresponds to an ^{31}P–^{27}Al distance of 2.93 Å. First, one can note that maximum peak intensity occurs at a value $\tau_p + \tau_d$ equal to the rotor period τ_R. One can note that a slight dip appears with increasing values of τ_p. This dip in itself cannot however explain the significant dip observed in the experimental data. This small dip corresponds to the fact that when the pulse length becomes long enough, adiabatic transfers occur during the pulse, which affect certain crystallites. This leads to a slight dipolar recoupling that increases with τ_p.

The second simulation (Fig. 6b) was conducted by considering this time a scalar coupling of 30 Hz in the ^{31}P–^{27}Al spin system. In this case, the calculated intensity is basically constant except for the exact synchronisation condition for which we observe a dramatic intensity drop. This result can be interpreted by the fact that the pulses, which then occur at each rotor period, affect the same crystallites in a systematic way, and continuously throughout the 40 ms ^{31}P acquisition time. Hence, one can consider that under these conditions only a limited amount of crystallites are affected by the scalar decoupling. However, as soon as $\tau_p + \tau_d$ slightly deviates from τ_R, the rotor-asynchronisation ensures that throughout the ^{31}P acquisition time, all crystallites are affected by the scalar decoupling. Fig. 6c reports the calculation of the spin system when it is subjected to both dipolar and scalar interactions. The simulation presents rather truthfully the pattern of the experimental results shown in Fig. 5.

4. Conclusion

We have presented a new and important sequence that provides the means to augment significantly the spectral resolution through the scalar decoupling of a quadrupolar nucleus. In the rotor-synchronised version, this new sequence avoids the dipolar recoupling that was observed when using the classical CW decoupling sequence. Our sequence also provides the advantage of being only slightly dependent on offset and to minimize the Bloch–Siegert

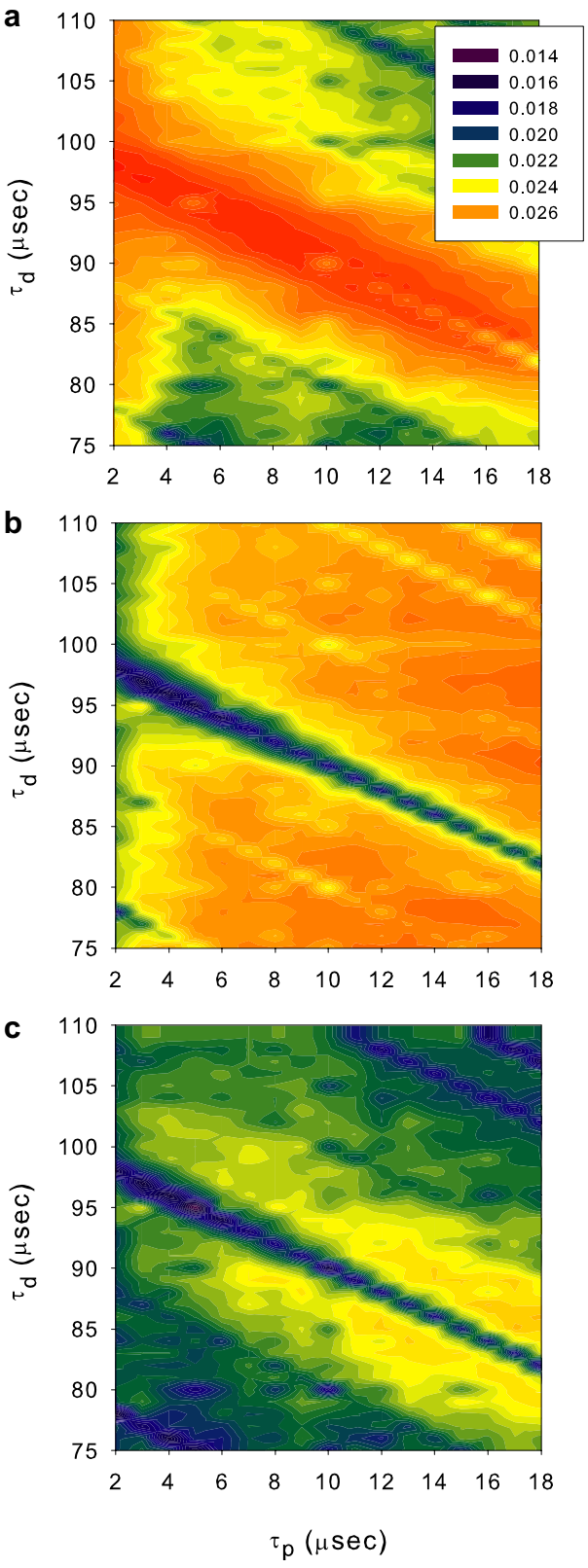

Fig. 6. SIMPSON simulations. The quadrupolar constant C_Q was 3 MHz, asymmetry parameter η_Q was 0. (a) the ^{31}P–^{27}Al dipolar coupling (500 Hz) only was considered in the calculation. (b) the ^{31}P–^{27}Al J coupling of 30 Hz was considered. (c) corresponds to the experimental case where the quadrupolar, dipolar and J couplings are taken into account ($\nu_1^{Al} = 70$ kHz).

shift. We have furthermore shown that the experimental setting for optimal resolution was found for slightly rotor-asynchronised decoupling period. Numerical simulations confirmed our results and provided the means to demonstrate the effect of perfect synchronisation on scalar coupling. The RA-MP decoupling sequence has yet another advantage over the rotor-synchronised version. Indeed, it is less demanding upon the power dissipation within the probe circuitry i.e the decoupling duty cycle is much smaller in the case of asynchronisation compared to the case of synchronised condition. Consequently, this feature gave us the mean to increase the decoupling rf field amplitude in order to reach even better resolution (see Fig. 2d). In conclusion, our results argue in favour of a systematic use of RA-MP decoupling sequences when the observed nucleus is chemically bonded to a quadrupolar nucleus with a high natural abundance.

Acknowledgments

Authors would like to thank Region Nord/Pas de Calais, Europe (FEDER), CNRS, French Minister of Science, USTL, ENSCL, and the Bruker company for funding. We also would like to acknowledge Florian Paviot for his help on simulations.

References

[1] A.J. Shakaa, James Keeler, Broadband spin decoupling in isotropic-liquids, Prog. Nucl. Magn. Reson. Spectrosc. 19 (1987) 47–129.
[2] M.A. Mc Coy, L. Mueller, Selective decoupling, J. Magn. Reson. A 101 (1993) 122–130.
[3] E. Kupce, R. Freeman, Adiabatic pulses for wideband inversion and broadband decoupling, J. Magn. Reson. A 115 (1995) 273–276.
[4] C.J. Besecker, W.G. Klemperer, D.J. Maltbie, D.A. Wright, ^{17}O Nuclear magnetic resonance spectroscopy of polyoxometalates. 2. Heteronuclear decoupling of quadrupolar nuclei, Inorg. Chem. 24 (1985) 1027–1032.
[5] S.A. Smith, N. Murali, Relaxation effects in a system of a spin-1/2 nucleus coupled to a quadrupolar spin subjected to RF irradiation: Evaluation of broadband decoupling schemes, J. Magn. Reson. 136 (1999) 27–36.
[6] P. Bendel, A. Baram, Line narrowing of $I = 1/2$ spins coupled to quadrupolar nuclei in liquids: Effects of weak decoupling fields, J. Magn. Reson. 141 (1999) 121–132.
[7] A.E. Bennett, C.M. Rienstra, M. Auger, K.V. Lakshmi, R.G. Griffin, Heteronuclear decoupling in rotating solids, J. Chem. Phys. 103 (1995) 6951–6958.
[8] A. Detken, E.H. Hardy, M. Ernst, B.H. Meier, Simple and efficient decoupling in magic-angle spinning solid-state NMR: the XiX scheme, Chem. Phys. Lett. 356 (2002) 298–304.
[9] B.M. Fung, A.K. Khitrin, K. Ermolaev, An improved broadband decoupling sequence for liquid crystals and solids, J. Magn. Reson. 142 (2000) 97–101.
[10] Z.H. Gan, R.R. Ernst, Frequency- and phase-modulated heteronuclear decoupling in rotating solids, Solid State NMR 8 (1997) 153–159.
[11] A.K. Khitrin, T. Fujiwara, H. Akutsu, Phase-modulated heteronuclear decoupling in NMR of solids, J. Magn. Reson. 162 (2003) 46–53.
[12] G.D. Paeÿpe, D. Sakellariou, P. Hodgkinson, S. Hediger, L. Emsley, Heteronuclear decoupling in NMR of liquid crystals using continuous phase modulation, Chem. Phys. Lett. 368 (2003) 511–522.
[13] G. De Paëpe, P. Hodgkinson, L. Emsley, Improved heteronuclear decoupling schemes for solid-state magic angle spinning NMR by direct spectral optimization, Chem. Phys. Lett. 376 (2003) 259–276.
[14] K. Riedel, J. Leppert, O. Ohlenschlaĝer, M. Goŕlach, R. Ramachandran, Heteronuclear decoupling in rotating solids via symmetry-based adiabatic RF pulse schemes, Chem. Phys. Lett. 395 (2004) 356–361.
[15] X. Filip, C. Tripon, C. Filip, Heteronuclear decoupling under fast MAS by a rotor-synchronized Hahn-echo pulse train, J. Magn. Reson. 176 (2005) 239–243.
[16] R.S. Thakur, N.D. Kurur, P.K. Madhu, Swept-frequency two-pulse phase modulation for heteronuclear dipolar decoupling in solid-state NMR, Chem. Phys. Lett. 426 (2006) 459–463.
[17] S. Hafner, A. Palmer, M. Cormos, Pulsed heteronuclear decoupling under ultra-fast magic-angle spinning, in: 47th ENC Conference, 23–28 April 2006, Poster P184.
[18] R.M. Orr, M.J. Duer, Decoupling residual dipolar coupling between ^{13}C and ^{14}N spin pairs in CPMAS NMR, Solid State Nucl. Magn. Reson. 30 (2006) 130–134.
[19] R.W. Schurko, R.E. Wasylishen, J.H. Nelson, Effect of Cobalt-59 self-decoupling on the solid-state ^{31}P CP/MAS NMR spectra of cobaloximes, J. Phys. Chem. 100 (1996) 8057–8060.
[20] D. Christendat, R. Markwell, D. Gilson, I. Butler, J. Cotton, Quadrupole-dipole effects in solid-state Phosphorus-31, CP-MAS NMR spectra of tertiary phosphine substituted Alkyl- and Acyltetracarbonylmanganese(I), complexes, Inorg. Chem. 36 (1997) 230–235.
[21] K. Eichele, R.E. Wasylishen, J.H. Nelson, Solid-State ^{95}Mo NMR studies of some prototypal molybdenum compounds: Sodium molybdate dihydrate, hexacarbonylmolybdenum, and pentacarbonyl phosphine molybdenum(0) complexes, J. Phys. Chem. A 101 (1997) 5463–5468.
[22] H. Heise, F.H. Köhler, E.B. Brouwer, R.K. Harris, Stefan Steuernagel, ^{59}Co second-order quadrupolar effects in the ^{13}C cross-polarization magic angle spinning NMR spectra of the cobaltocenium salts $[Cp^*_2Co]Y[PF_6]^-$ and $[Cp^*CpCo]Y[PF_6]^-$, Magn. Reson. Chem. 37 (1999) 573–578.
[23] L. Du, R.W. Schurko, K.H. Lim, C.P. Grey, A solid-state ^{93}Nb and ^{19}F NMR spectroscopy and X-ray diffraction study of potassium heptafluoroniobate(V): Characterization of ^{93}Nb, ^{19}F coupling, and fluorine Mo, J. Phys. Chem. A 105 (2001) 760–768.
[24] H-M. Kao, K-H. Lii, The first observation of heteronuclear two-bond J-coupling in the solid state: crystal structure and solid-state NMR spectroscopy of $Rb_4(NbO)_2(Si_8O_{21})$, Inorg. Chem. 41 (2002) 5644–5646.
[25] L. Delevoye, C. Fernandez, C. Morais, J-P. Amoureux, V. Montouillout, J. Rocha, Double-resonance decoupling for resolution enhancement of ^{31}P solid-state MAS and ^{27}Al ^{31}P MQHETCOR NMR, Solid State Nucl. Magn. Reson. 22 (2002) 501–512.
[26] R.W. Broach, S.T. Wilson, R.M. Kirchner, Corrected crystallographic tables and figure for as-synthesized $AlPO_4$-14, Micropor. Mesopor. Mater. 57 (2003) 211–214.
[27] M. Bak, J.T. Rasmussen, N.C. Nielsen, SIMPSON: A general simulation program for solid state NMR spectroscopy, J. Magn. Reson. 147 (2000) 296–330.
[28] C.P. Grey, W.S. Veeman, A.J. Vega, Rotational echo ^{14}N/^{13}C/^{1}H triple resonance solid state nuclear magnetic resonance: A probe of ^{13}C-^{14}N internuclear distances, J. Chem. Phys. 98 (1993) 7711–7724.
[29] T. Gullion, Measurement of dipolar interactions between spin-1/2 and quadrupolar nuclei by rotational-echo, adiabatic-passage, double-resonance NMR, Chem. Phys. Lett. 246 (1995) 325–330.
[30] T. Gullion, D.B. Baker, M.S. Conradi, New, compensated Carr-Purcell sequences, J. Magn. Reson. 89 (1990) 479–484.
[31] F. Bloch, A. Siegert, Magnetic resonance for nonrotating fields, Phys. Rev. 57 (1940) 522–527.
[32] S.A. Vierkötter, Applications of the Bloch–Siegert shift in solid state proton-dipolar-decoupled ^{19}F MAS NMR, J. Magn. Reson. A 118 (1996) 84–93.